Error bounds on diffusive flow models from noisy microseismic data

Oleg V. Poliannikov[*†], *Michael Fehler*[†], *and Alison E. Malcolm*[‡]
[†] *Earth Resources Laboratory, Department of EAPS, Massachusetts Institute of Technology*
[‡] *Earth Sciences Department, Memorial University of Newfoundland*

SUMMARY

We study the effect of the uncertainty in the induced microseismic event locations and origin times on the inverted fluid pressure diffusivity. We use a probabilistic physical model that directly ties fluid pressure in the subsurface during the injection to observations of induced microseismic events at the monitoring receiver array to track the propagation of uncertainty in the forward model and inversion. We use this model to invert for fluid pressure during injection from synthetically modeled noisy travel times and an uncertain velocity model, and to quantify the uncertainty of this inversion. Examples presented provide evidence that reliable inversion of fluid flow parameters from observed microseismic data with uncertainty quantification is possible.

INTRODUCTION

Hydraulic fracturing is the primary tool to increase productivity of unconventional reservoirs (Jones and Britt, 2009). Despite its pervasive use, hydraulic fracturing is often inefficient due to the lack of comprehensive diagnostics to characterize the fracture network created. A better understanding of the relationship between the fluid flow during the injection and the observed microseismic data would increase the value of microseismic monitoring and likely lead to more efficient fracturing operations.

Poliannikov et al. (2015) have developed a probabilistic model that ties fluid pressure during injection to observed microseismicity. This model uses a Bayesian formulation that accounts for the uncertainties associated with rock cohesion, rock friction, and the maximum and minimum stresses of the formation, which are dominant factors controlling induced rock failure and the associated microseismicity. Their analysis can be used to predict general patterns of microseismicity induced by the injected fluid, and to invert for the pressure diffusivity of the subsurface from the induced microseismicity. However, in their numerical examples observations of microseismic events and origin times were assumed to be known or recovered without errors.

In this paper, we study the effect of uncertainty in estimated microseismic events and origin times on the quality of inversion of pressure diffusivity. Because event locations are estimated by ray-tracing using an assumed velocity model and comparing predicted arrival times with the recorded traveltime data, the effect of the velocity uncertainty on the uncertainty in the event locations and origin times is quite pronounced. A natural question then becomes: Will the uncertainty in the velocity model render it impossible to use observed microseismicity to draw inferences about fluid flow in the subsurface?

We present evidence to show that despite the presence of noise in the data and velocity uncertainty, we can under favorable circumstances obtain reliable estimates of the parameters controlling fluid pressure during the injection.

EFFECTIVE-DIFFUSION FLOW

We consider a two-dimensional radially symmetric medium around the injection point (Figure 1) (Shapiro et al., 2005). We model the fluid pressure in the formation as an effective (upscaled) diffusion, which is a good model for a variety of field settings. Even when the rock matrix is virtually impermeable, fluid pressure may still diffuse at a larger scale through many connected fractures. The upscaled effective diffusivity accounts for possible fractures and fracture networks on the large scale (Shapiro et al., 2000).

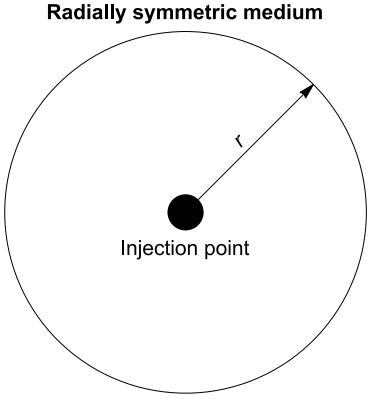

Figure 1: *Our model is a radially symmetric medium that is centered on the point of injection.*

Denoting by r the radial distance from the injection point, we assume that fluid is injected into a medium with a non-homogeneous isotropic diffusivity, $\alpha(r)$, at the rate, $R(r,t)$ as shown in Figure 2.

The pressure field (above the initial background level) $p(r,t)$ at distance r and time t is governed by the initial-value boundary-value problem (Shapiro et al., 2002, 2005):

$$\begin{cases} \dfrac{\partial p(r,t)}{\partial t} = \nabla \cdot [\alpha(r)\nabla p(r,t)] + R(r,t) \\ p(r,0) = 0 \\ \dfrac{\partial}{\partial r} p(0,t) = 0,\ p(\infty,t) = 0. \end{cases} \tag{1}$$

DOI http://dx.doi.org/10.1190/segam2015-5866978.1

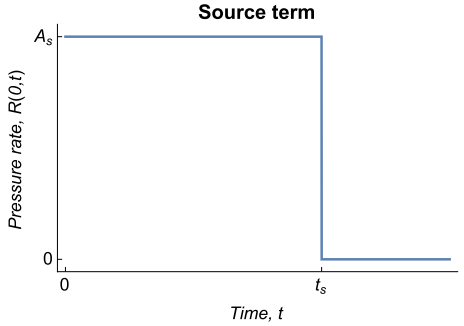

Figure 2: *Injection rate at the location $r = 0$; this is the source term in Equation 1. In subsequent examples, $A_s = 1$ and $t_s = 1$.*

As a result of the injection, the fluid pressure within the medium, $p(r,t)$, increases from $t = 0$ until it reaches its maximum value at some time $t_{\max}(r \mid \alpha) \geq t_s$, which depends on both the location and the diffusivity, and then drops and decays to zero as $t \to \infty$ as shown in Figure 3. Knowing the maximum pressure at any given location enables us to determine the likelihood of rock fracture. To find $t_{\max}(r \mid \alpha)$, we numerically solve for the extremum of the solution to the diffusion equation:

$$\frac{\partial}{\partial t} p(r,t \mid \alpha)\Big|_{t=t_{\max}(r|\alpha)} = 0. \tag{2}$$

The maximum pressure, $p_{\max}(r \mid \alpha)$, attained at a distance r is calculated by plugging $t_{\max}(r \mid \alpha)$ into the solution to Equation 1, *i.e.*,

$$p_{\max}(r \mid \alpha) \equiv p(r, t_{\max}(r \mid \alpha) \mid \alpha). \tag{3}$$

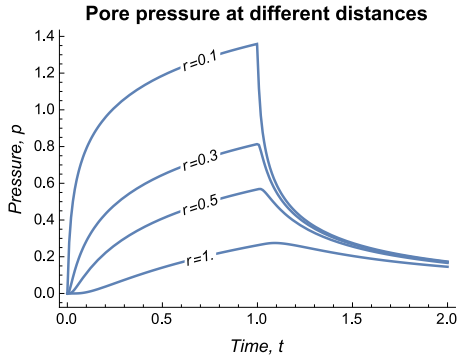

Figure 3: *Sample pressure profiles that are solutions to Equation 1, for a fixed diffusivity, $\alpha(r) \equiv 1$, and different locations, r.*

ROCK FAILURE MODEL BACKGROUND

Pressure at rock failure

Following Poliannikov et al. (2015), we characterize the physical properties of the subsuface by a set of four model parameters. At each distance from the injection point, r_i, the medium can be described by four parameters that control rock failure:

$$m_i = \{\sigma_c(i), \kappa(i), \sigma_1(i), \sigma_3(i)\}, \tag{4}$$

where σ_c is the rock cohesion, κ is the rock friction, σ_1 is the maximum principal stress, and σ_3 is the minimum principal stress (Ottosen and Ristinmaa, 2005). Here we will assume that the distances $\{r_i\}$ are chosen such that all four parameters at different locations are statistically independent.

Time of failure

According to the classical Mohr-Coulomb theory (von Terzaghi, 1943), increasing fluid pressure reduces the effective stress and, upon reaching a critical level, causes failure. This corresponds to the Mohr circle touching the Coulomb failure envelope at one point (Figure 4). The pressure level that is necessary to cause a rock failure at distance r_i will be called the pressure at failure and denoted $p_{\text{fail}}(i)$.

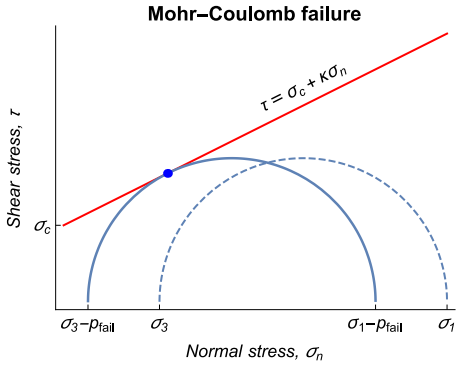

Figure 4: *Pressure, p, rises until it reaches the level $p = p_{\text{fail}}$ when Mohr's circle (blue) touches the Coulomb failure envelope (red) and a failure occurs.*

If the four parameters, $\{\sigma_c, \kappa, \sigma_1, \sigma_3\}$, of the model and fluid pressure are known exactly, then rock failure is directly linked to pore pressure, and hence to diffusivity (Poliannikov et al., 2015). When the four parameters carry uncertainty and hence are described by probability distributions, a failure may or may not occur depending on a particular realization of these parameters (Figure 5).

This framework allows us to forecast a probability distribution for microseismic events given the uncertain parameters $\{\sigma_c, \kappa, \sigma_1, \sigma_3\}$ in the subsurface. For each distance r_i across some *a priori* chosen grid, we can determine the probability of a failure, $P_{\text{fail}}(r_i \mid \alpha)$, at the location, r_i, and, if applicable, the probability distribution of its time, $f_{t_{\text{fail}}(r_i|\alpha)}(t)$.

The probability $P_{\text{fail}}(r_i \mid \alpha)$ is specific to each given distance and diffusivity. It is computed as follows:

$$P_{\text{fail}}(r_i \mid \alpha) \quad = \quad F_{p_{\text{fail}}(i)}\left(p_{\max}(r_i \mid \alpha)\right), \tag{5}$$

where $\mathbb{P}[\cdot]$ denotes probability, and $F_{p_{\text{fail}}(i)}(p) \equiv \mathbb{P}[p_{\text{fail}}(i) \leq p] = \int_{-\infty}^{p} f_{p_{\text{fail}}(i)}(p')\,dp'$ is the cumulative distribution function for $p_{\text{fail}}(i)$, the pressure at failure that can be easily computed from assumed distributions of the model parameters m_i.

DOI http://dx.doi.org/10.1190/segam2015-5866978.1

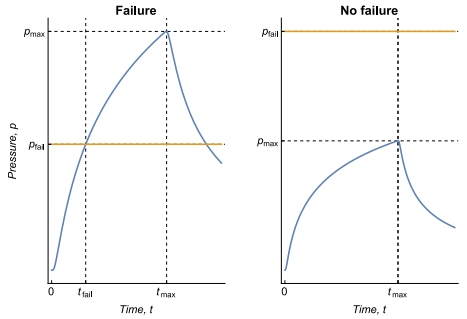

Figure 5: *(left) A failure occurs if the pressure, $p(r,t)$, at a given location, r, reaches the required level, p_{fail}. The maximum pressure then by definition equals or exceeds this level. (right) If the pressure, $p(r,t)$, never reaches the level, p_{fail}, then no failure occurs at this location.*

The time of failure, $t_{\text{fail}}(r_i \mid \alpha)$, if the failure occurs, is a random variable whose distribution is described by a probability density function, $f_{t_{\text{fail}}(r_i|\alpha)}(t)$ (Poliannikov et al., 2015):

$$f_{t_{\text{fail}}(r_i|\alpha)}(t) \quad = \quad \frac{f_{p_{\text{fail}}(i)}\left(p(r_i,t \mid \alpha)\right) \frac{\partial}{\partial t} p(r_i,t \mid \alpha)}{F_{p_{\text{fail}}(i)}\left(p_{\max}(r_i \mid \alpha)\right)}, \tag{6}$$

when $t \in [0, t_{\max}(r_i \mid \alpha)]$, and zero otherwise. In practice, many microseismic events are observed after $t_{\max}(r_i \mid \alpha)$, but since our focus here is on microseismic triggering fronts, these later events are not considered.

Figure 6 shows an example of a simulated induced microseismicity. There we assume that all parameters except the minimum stress σ_3 are known. The minimum stress is assumed to be known up to an error of $\pm 5\%$.

PROBABILISTIC INVERSION FROM UNCERTAIN EVENT LOCATIONS

Consider first the problem of inverting for the diffusivity, α, from perfectly known event locations and origin times that we summarily denote by s. Poliannikov et al. (2015) show that the posterior distribution of the diffusivity is given by

$$f(\alpha \mid s) \quad \propto \quad \prod_{i=1}^{N_{\text{events}}} f_{t_{\text{fail}}(r_i|\alpha)}(t_i)\, P_{\text{fail}}(r_i \mid \alpha) \tag{7}$$

where we have assumed uninformed (flat) prior distribution of the diffusivity. In Figure 7 we show the posterior density function of the diffusivity, α, given the microseismicity shown in Figure 6.

In field applications, microseismic event locations and origin times are not observed directly. Instead they are estimated with some uncertainty from recorded microseismic data (Michaud et al., 2004; Bennett et al., 2005; Huang et al., 2006; Poliannikov et al., 2013, 2014). Uncertainty in the estimated event locations and origin times depends on several factors, receiver array geometry, velocity uncertainty and signal noise being among the most

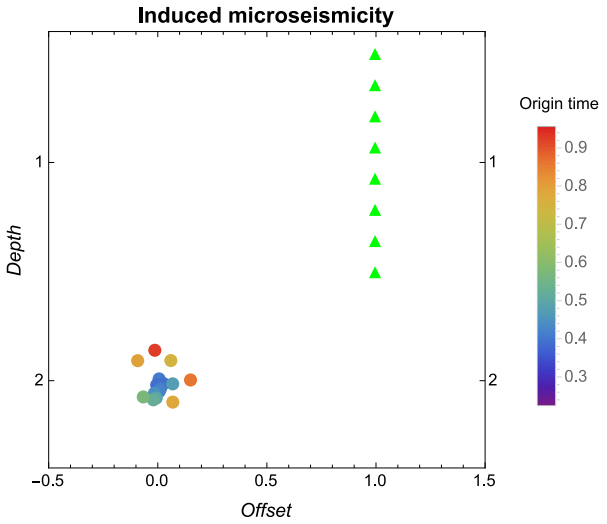

Figure 6: *A simulated realization of the induced microseismicity caused by an injection at the point $(0,2)$. Each microseismic event is recorded by a borehole receiver array located nearby (green triangles).*

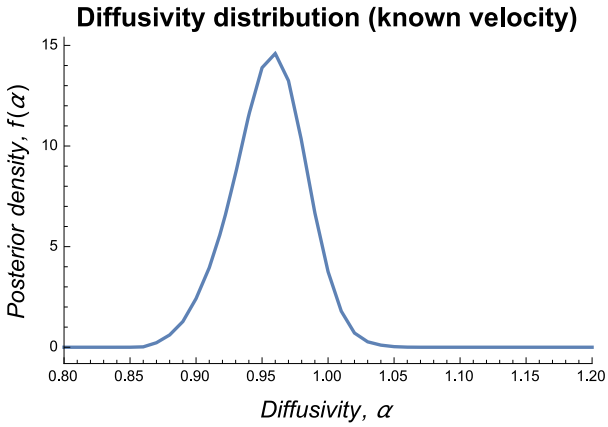

Figure 7: *The posterior distribution of the diffusivity, α, given the observed microseismicity in Figure 6, the flat (completely uninformed) prior, and assumptions about the physical parameters of the medium. The uncertainty in the α is due to the uncertainty in the minimum stress σ_3. Because the event locations and origin times are assumed known, velocity uncertainty has no effect on the posterior of α.*

important. Here we demonstrate that in some cases the diffusivity can be recovered from noisy arrival times.

First, denote by T the observed travel-time data, α the unknown diffusivity, and s the true microseismic event locations and origin times. Then we have (Poliannikov et al., 2015):

$$f(\alpha \mid T) \quad = \quad \int f(s \mid T)\, f(\alpha \mid s)\, \mathrm{d}s, \tag{8}$$

where $f(s \mid T)$ is the joint probability density function of event locations *and* times, given observed travel times (Poliannikov et al., 2013, 2014), and $f(\alpha \mid s)$ is the posterior of diffusivity given

DOI http://dx.doi.org/10.1190/segam2015-5866978.1

microseismic events as computed above.

Figure 8 shows the result of the inversion for the pressure diffusivity using the noisy travel times from the microseismic events shown in Figure 6 and a homogeneous velocity model with uncertainty of $\pm 5\%$. The signal noise is assumed to be independent Gaussian with a standard deviation of $\sigma = 10^{-3}$.

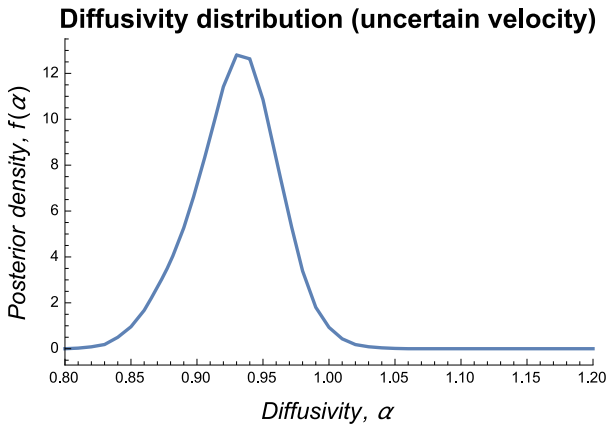

Figure 8: *The posterior distribution of the diffusivity, α, given observed noisy travel times and an uncertain velocity model.*

By comparing the posterior distributions in Figures 7 and 8, we can see that the uncertainty has not increased dramatically. This result, of course, is obtained for a specific experiment and is not representative of all possible models of fluid flow, rock fracture, and all monitoring geometries. However, it is important to consider reasons for relatively good inversion results in this particular case.

Equation 8 has two key ingredients: a joint probability distribution of locations and times of induced microseismic events and a posterior distribution of the diffusivity given a particular realization of event locations and times. Both ingredients help control the uncertainty in the inverted diffusivity.

It is well-known that locating microseismic events one-by-one involves a trade-off between an (uncertain) velocity and the event location and origin time and may lead to a poorly constrained event. The joint (simultaneous) location of multiple events at the same time is a much better constrained problem. The relative location of one event with respect to others is less sensitive to velocity perturbations, and the absolute locations of all events are often highly correlated (Waldhauser and Ellsworth, 2000; Zhang and Thurber, 2003; Poliannikov et al., 2011, 2013). Large velocity deviations, for example, are ruled out by the posterior because they are incompatible with the observed arrival times from all recorded microseismic events. This phenomenon is widely used in velocity estimation using microseismic events. Here we do not need to explicitly estimate the velocity model because only good velocity models contribute significantly to the posterior.

Consider now a family of jointly located microseismic events. They can be thought of as random samples of all event locations and origin times such that each sample is consistent with the observed travel-time data and prior assumptions about the velocity uncertainty and signal noise. According to the flow model and rock failure mechanism described above, microseismic events must propagate away from the known injection point isotropically in a diffusive fashion with the square-root of the origin time being proportional to the distance of the event from the injection point. Some realizations of the event locations and event origin times will be inconsistent with the rock failure model, *i.e.*, highly unlikely, for any choice of the flow diffusivity. The contributions of these microseismicity realizations to the diffusivity posterior inside Equation 8 will be very small.

CONCLUSIONS

In this paper we presented a model physically tying together fluid pressure during injection to observed uncertain direct arrival times of the induced microseismic events. This physical model gave rise to a probabilistic model that could be used for forward predictions and inversions. We inverted for the effective diffusivity of the fracture system during injection from the observed travel times using an uncertain velocity model and prior assumptions about signal noise and rock physics parameters in the subsurface. We used a simple numerical example to demonstrate that the velocity uncertainty being one of the largest factors of uncertainty in earthquake location might have a limited effect on the inverted diffusivity if the inversion was performed optimally.

AKNOWLEDGEMENTS

We thank Michael Prange of Schlumberger-Doll Research and Hugues Djikpesse for useful discussions.

DOI http://dx.doi.org/10.1190/segam2015-5866978.1

EDITED REFERENCES

Note: This reference list is a copyedited version of the reference list submitted by the author. Reference lists for the 2015 SEG Technical Program Expanded Abstracts have been copyedited so that references provided with the online metadata for each paper will achieve a high degree of linking to cited sources that appear on the Web.

REFERENCES

Bennett, L., J. Le Calvez, D. R. Sarver, K. Tanner, W. S. Birk, G. Waters, J. Drew, G. Michaud, P. Primiero, L. Eisner, R. Jones, D. Leslie, M. J. Williams, J. Govenlock, R. C. Klem, and K. Tezuka, 2005, The source for hydraulic fracture characterization: Oilfield Review, **17**, no. 4, 42–57.

Huang, Y. A., J. Benesty, and J. Chen, 2006, Acoustic MIMO signal processing: Springer.

Jones, J. R., and L. K. Britt, 2009, Design and appraisal of hydraulic fractures: Society of Petroleum Engineers.

Michaud, G., D. Leslie, J. Drew, T. Endo, and K. Tezuka, 2004, Microseismic event localization and characterization in a limited aperture HFM experiment: 74th Annual International Meeting, SEG, Expanded Abstracts, 552–555.

Ottosen, N. S., and M. Ristinmaa, 2005, The mechanics of constitutive modeling: Elsevier.

Poliannikov, O. V., A. E. Malcolm, H. Djikpesse, and M. Prange, 2011, Interferometric hydrofracture microseism localization using neighboring fracture: Geophysics, **76**, no. 6, WC27–WC36, http://dx.doi.org/10.1190/geo2010-0325.1.

Poliannikov, O. V., M. Prange, H. Djikpesse, A. E. Malcolm, and M. Fehler, 2015, Bayesian inversion of pressure diffusivity from microseismicity: Geophysics, **80**, no. 4, M43–M52, http://dx.doi.org/10.1190/geo2014-0374.1.

Poliannikov, O. V., M. Prange, A. E. Malcolm, and H. Djikpesse, 2013, A unified Bayesian framework for relative microseismic location: Geophysical Journal International, **194**, no. 1, 557–571, http://dx.doi.org/10.1093/gji/ggt119.

Poliannikov, O. V., M. Prange, A. E. Malcolm, and H. Djikpesse, 2014, Joint location of microseismic events in the presence of velocity uncertainty: Geophysics, **79**, no. 6, KS51–KS60.

Shapiro, S. A., P. Audigane, and J.-J. Royer, 2000, Reply to comment by F. H. Cornet on 'Large-scale *in situ* permeability tensor of rocks from induced microseismicity': Geophysical Journal International, **140**, no. 2, 470–473.

Shapiro, S. A., S. Rentsch, and E. Rothert, 2005, Characterization of hydraulic properties of rocks using probability of fluid-induced microearthquakes: Geophysics, **70**, no. 2, F27–F33.

Shapiro, S. A., E. Rothert, V. Rath, and J. Rindschwentner, 2002, Characterization of fluid transport properties of reservoirs using induced microseismicity: Geophysics, **67**, 212–220, http://dx.doi.org/10.1190/1.1451597.

Terzaghi, K., 1943, Theoretical soil mechanics: John Wiley & Sons, Ltd., http://dx.doi.org/10.1002/9780470172766.

Waldhauser, F., and W. L. Ellsworth, 2000, A double-difference earthquake location algorithm: Method and application to the northern Hayward fault, California: Bulletin of the Seismological Society of America, **90**, no. 6, 1353–1368, http://dx.doi.org/10.1785/0120000006.

Zhang, H., and C. H. Thurber, 2003, Double-difference tomography: The method and its application to the Hayward fault, California: Bulletin of the Seismological Society of America, **93**, no. 5, 1875–1889, http://dx.doi.org/10.1785/0120020190.